Int J Ind Chem (2017) 8:315–327
DOI 10.1007/s40090-017-0121-4

RESEARCH

# Properties of complex ammonium nitrate-based fertilizers depending on the degree of phosphoric acid ammoniation

**Konstantin Gorbovskiy[1] · Anatoly Kazakov[2] · Andrey Norov[1] · Andrey Malyavin[1] · Anatoly Mikhaylichenko[3]**

Received: 25 June 2016 / Accepted: 20 March 2017 / Published online: 3 April 2017


**Abstract** Complex ammonium nitrate-based NP and NPK fertilizers are multicomponent salt systems prone to high hygroscopicity, caking and explosive thermal decomposition. The slurries that used in the production of these fertilizers can also exhibit insufficient thermal stability. One of the most important issues for such slurries is their viscosity, which determines the energy costs for transportation and processing into the final product. Increasing the degree of phosphoric acid ammoniation helps to reduce the ammonium nitrate's content in the product, but the main question remains about the properties of such fertilizers. This article is devoted to studying properties of complex NP and NPK ammonium nitrate-based fertilizers and their intermediates with increasing the degree of phosphoric acid ammoniation.

**Keywords** Ammonium nitrate-based fertilizer · Hygroscopicity · Caking · Microcalorimetry · Thermal decomposition · Slurry viscosity

✉ Konstantin Gorbovskiy
sulfur32@bk.ru

[1] The Research Institute for Fertilizers and Insecto-Fungicides Named after Professor Y. Samoilov, 162622 Cherepovets, Vologda Region, Russia

[2] Institute of Problems of Chemical Physics of the Russian Academy of Sciences, 142432 Chernogolovka, Moscow Region, Russia

[3] D. Mendeleev University of Chemical Technology of Russia, 125047 Moscow, Russia

## Introduction

Ammonium nitrate (AN) is one of the most common commercially available nitrogen fertilizers, the content of nitrogen in which amounts up to 35% by mass. The main agrochemical advantage of AN compared to other simple nitrogen fertilizers is to present nitrogen both in ammonia and nitrate forms. Herewith, the high content of this component enables to mix it with other types of fertilizers and obtain complex fertilizer with the high content of basic nutrients—nitrogen, phosphorus and potassium. The main disadvantages of such types of fertilizers are their high hygroscopicity, caking [1] and the increased requirements for fire and explosion safety [2]. All the above-mentioned factors, and in particular the last, are the main disadvantages limiting the production of complex AN-based fertilizers.

Cases of explosion of AN and complex AN-based fertilizers are well known: in 1921 in the warehouse in Oppau (Germany), in 1947 in the warehouse in the bay in Texas City (USA), in 2001 in the warehouse in Toulouse (France), in 2013 in the warehouse in West (USA). The largest explosion of technological installations was recorded in 1952 in Nagoya (Japan), in 1978—in Chirchik (Uzbekistan) in 1981—in Cherepovets (Russia), in 1994—in Port Neil (USA), in 2009—in Kirovo-Chepetsk (Russia).

Ammonium phosphates $NH_4H_2PO_4$ and $(NH_4)_2HPO_4$, ammonium sulfate and potassium chloride are also used in the production of complex AN-based NPK fertilizers. Herewith, the following reactions take place:

$$NH_4H_2PO_4 + KCl \rightleftarrows KH_2PO_4 + NH_4Cl, \quad (1)$$

$$NH_4NO_3 + KCl \rightleftarrows KNO_3 + NH_4Cl, \quad (2)$$

$$(NH_4)_2SO_4 + 2KCl \rightleftarrows K_2SO_4 + 2NH_4Cl. \quad (3)$$

$KH_2PO_4$, $KNO_3$ and $K_2SO_4$ in combination with unreacted $NH_4H_2PO_4$, $NH_4NO_3$ and $(NH_4)_2SO_4$ (accordingly) form solid solutions—compounds of isomorphic-substituted type.

The composition of the solid solutions is determined by the extent of the conversion of the reactions (1–3). $(NH_4)_2HPO_4$ does not react with KCl. Moreover, AN can form various double salts: $NH_4NO_3{\cdot}2KNO_3$, $(NH_4)_2SO_4{\cdot}2NH_4NO_3$, $(NH_4)_2SO_4{\cdot}3NH_4NO_3$. Formation of $NH_4NO_3{\cdot}2KNO_3$ depends on the extent of the conversion of the reaction (2) [3]. The double salts $(NH_4)_2SO_4{\cdot}2NH_4NO_3$ and $(NH_4)_2SO_4{\cdot}3NH_4NO_3$ in the presence of KCl can decompose with the formation of solid solutions [4].

Thus, complex AN-based fertilizers are complex salt systems, whose composition is defined by the ratio of initial components.

The presence of all the above-mentioned compounds can variously affect the decomposition of complex AN-based fertilizers and their propensity for detonation. The presence of $NH_4H_2PO_4$, $(NH_4)_2HPO_4$ and $(NH_4)_2SO_4$ reduces the rate of AN decomposition [5, 6], and chloride-anions $Cl^-$, on the contrary, act as catalysts for AN decomposition [7–9].

Despite this, increasing demands of the agrochemical sector leads to the necessity to develop new grades of the fertilizers, the production of which is possible only when using concentrated nitrogen fertilizers, especially ammonium nitrate and urea. However, considerable difficulties emerge in case of urea used, which consist in high hygroscopicity and caking, reduction of the amide nitrogen proportion in the product due to decomposition of urea at relatively low temperatures during granulation and drying, and complexity of the technological process because of heavy clogging of equipment [10, 11].

One of the ways to improve the quality of complex AN-based fertilizers and reduce the risk of explosion is to increase the ammoniation degree of wet-process phosphoric acid, which reduces the AN portion in the product. Such way can improve the properties of the final product (decrease hygroscopicity and caking), increase its thermal stability, decrease the amount of different compounds in exhaust gases (nitrous gases, chlorine and fluorine compounds) during thermal decomposition, increase fire and explosion safety, and also decrease viscosity of ammonium phosphate–nitrate slurries produced during the production of fertilizer that can decrease energy cost for their transportation. However, information on influence of the degree of phosphoric acid ammoniation on the above-mentioned properties of complex AN-based fertilizers and their intermediates is absent in the literature.

Thus, the purpose of this work is to study the properties of complex AN-based fertilizers and intermediates in their production depending on the degree of phosphoric acid ammoniation.

## Experimental section

### Preparation of the samples

To produce complex fertilizers, concentrated hemihydrate phosphoric acid, nitric acid, ammonium sulfate and potassium chloride (mineral concentrate "Silvin") were used. Wet-process phosphoric acid was obtained from the Khibiny apatite concentrate (the Cola Peninsula, Russia) of composition: $P_2O_5$—51.72, CaO—0.67, MgO—0.23, F—1.33, $SO_3$—4.53, $Fe_2O_3$—0.55, $Al_2O_3$—0.90, $SiO_2$—0.43% by mass by sulfuric acid attack. Phosphoric and nitric acids were mixed in a certain ratio and ammoniated in a reactor equipped with the agitator device, the reflux condenser and the water jacket, which allowed ammoniation to be carried out under near-isothermal conditions at 70 ± 2 °C.

The degree of ammoniation of phosphoric acid $NH_3$:$H_3PO_4$ (M) was determined by pH value of the 1% by mass aqueous solution of the slurry obtained and using the reference source [12]. Ammonium sulfate and potassium chloride were introduced into the slurry in an amount necessary to obtain the desired grade, mixed thoroughly and dried at 65 °C. Then, the charge mixture was crushed and put in a pan granulator with diameter of 300 mm and length of 150 mm. Granules of 2–4 mm were finally dried at 65 °C to reach the required humidity. The product obtained was analyzed for content of basic elements.

### X-ray diffraction analysis

X-ray diffraction analysis of the investigated samples was performed when used powder diffractometer «STADI-MP» (STOE, Germany) with curved Ge (111) monochromator and radiation of $CuK_\alpha$ ($\lambda = 1.54056$ Å). The data acquisition was carried out in stepwise overlapping of scanning area mode by means of position-sensitive linear detector, the capture angle of which amounted 5° over $2\theta$ with channel width of 0.02°. The reliability and accuracy of compounds in X-ray patterns obtained were established by means of database of 2013 International Centre for Diffraction Data.

### Derivatographic analysis

Derivatographic analysis was carried out when used Paulik–Erdei derivatograph (MOM, Hungary) of Q-1500 series while heating in the air at atmospheric pressure in open quartz crucibles with heating rate of 2.5°/min. $Al_2O_3$ pre-

calcinated at 1000 °C was used as a reference. The sample weight amounted 0.2 g. The thermocouple was Pt/Pt–Pd. The interpretations of the dependencies obtained were carried out in compliance with the literature data [13–16].

### Hygroscopicity

Hygroscopicity ($K$) of the samples obtained was determined by means of climatic chamber BINDER KBF 115 (BINDER, Germany) with internal circulation. The value of $K$ was determined by means of conditioning of granule samples with the diameter of 3–4 mm with the mass of 3.500 ± 0.006 g in the chamber at 25 °C and the relative air humidity ($\varphi$) of 80% for 1 h. Granules were uniformly distributed in a cup with the diameter of 50 mm and height of 10 mm in a single layer. The value of $K$ was determined as the amount of water absorbed with a sample of unit mass for 1 h.

### Caking

Determination of caking ($\sigma$) of samples obtained was conducted by means of climatic chamber with internal circulation BINDER KBF 115 (BINDER, Germany) at temperature of 45 °C, $\varphi = 40\%$, and special presses equipped with calibrated spring. The spring load for each sample was 340 kPa. The samples detention time in the chamber was 6 h. Caking was determined as averaged maximum force required for breaking of formed cylindrical pellet divided by its cross-section area (pellet size: diameter 33 mm, height 40 mm).

### Static strength

Determining the static strength, $P$ was conducted by means of IPG-1M (Urals Scientific Research Institute of Chemistry with Experiment Plant, Russia) according to the formula:

$$P = \frac{\sum_{i=1}^{N} F_i}{\frac{\pi d_m^2}{4} N}, \quad (4)$$

where $F$ is the mean force required for breaking of one granule, $d_m$ is the mean diameter of one granule equal to 3.5 mm, and $N$ is the number of measured granules.

### Microcalorimetry

The microcalorimetric studies of the thermal decomposition kinetics were conducted by measuring the heat release rate in the samples under study with differential automatic calorimeter DAC-1-2 [17]. Tests were carried out in the vacuum-sealed glass ampoules with inner volume of about 2 $cm^3$, a mass of each tested mixture sample was 1 g. The free inner volume after putting each sample and sealing an ampoule was in the range 0.7–1.2 $cm^3$ per 1 g of the mixture tested. These ampoules were entirely put into the calorimeter and had no cold surfaces, and reaction products could not leave the boundaries of the reaction space.

### Gravimetric study of the thermal decomposition

Studies of mass loss in the thermal decomposition were conducted by maintaining granulated samples with mass of 20.00 ± 0.05 g in the electric oven without forced convection at the given temperature for a given period of time. The content of ammonium and nitrate nitrogen, chlorine, fluorine and sulfur was determined in products of the thermal decomposition. The fraction of these elements that have been released into the gas phase was calculated according to the formula:

$$X_A = \frac{\omega_0(\mathrm{A})\mathrm{m}_0 - \omega_\mathrm{t}(\mathrm{A})\mathrm{m}_\mathrm{t}}{m_0}, \quad (5)$$

where $X_A$ is the fraction of $A$ ($A = \mathrm{N_{amm}}$, $\mathrm{N_{nitr}}$, Cl, F) released into the gas phase per the unit mass of the initial sample; $\omega_0(A)$ is the mass fraction of $A$ in the initial sample; $m_0$ is the mass of the initial sample; $\omega_t(A)$ is the mass fraction of $A$ in the sample after the decomposition for time $t$; $m_t$ is the mass of the sample after the decomposition for a time $t$.

### Dynamic viscosity

The dynamic viscosity of slurries was determined by means of rotation viscometer HAAKE VT 74 Plus (Thermo Scientific, USA). In order to do that, the slurry obtained was placed in the cylindrical vessel provided with a thermostatic jacket and connected to circulation bath in which a polysilicon oil was circulated. After viscosity measurements, the slurry humidity was measured.

Processing experimental data obtained and the determination of confidence intervals for 95% confidence probability were conducted with the mathematical statistics methods by means of software application of origin.

## Results and discussion

### The composition of the fertilizer samples and X-ray diffraction analysis

Table 1 shows the results of analyses of fertilizer samples.

Figure 1 shows X-ray patterns for samples 1 and 2 (grade 26:13:0), 3 and 4 (grade 22:11:11), 5 and 6 (grade 16:16:16).

**Table 1** The composition of the fertilizer samples (%mass.)

| Sample no. | Grade | $N_{amm}$ | $N_{nitr}$ | $P_2O_5$ | S | $K_2O$ | *M* | $H_2O$ |
|---|---|---|---|---|---|---|---|---|
| 1 | 26:13:0 | 18.5 | 7.8 | 13.8 | 8.4 | – | 1.68 | 0.55 |
| 2 | | 15.8 | 10.1 | 13.3 | 4.2 | – | 1.06 | 0.42 |
| 3 | 22:11:11 | 14.9 | 7.6 | 11.4 | 5.6 | 11.4 | 1.71 | 0.59 |
| 4 | | 13.6 | 10.8 | 11.7 | 4.0 | 11.4 | 1.04 | 0.55 |
| 5 | 16:16:16 | 13.8 | 2.2 | 15.9 | 8.2 | 16.5 | 1.65 | 0.52 |
| 6 | | 12.3 | 4.0 | 16.5 | 4.0 | 16.4 | 1.07 | 0.48 |
| 7 | 20:10:10 | 16.0 | 3.9 | 9.9 | 11.0 | 10.3 | 1.70 | 0.53 |
| 8 | | 14.9 | 5.2 | 10.5 | 10.1 | 10.5 | 1.03 | 0.52 |
| 9 | 19:9:19 | 12.6 | 6.6 | 9.3 | 8.0 | 20.0 | 1.67 | 0.44 |
| 10 | | 11.6 | 8.2 | 9.3 | 2.8 | 20.3 | 1.03 | 0.51 |
| 11 | 27:6:6 | 16.4 | 10.9 | 6.4 | 2.6 | 6.5 | 1.66 | 0.49 |
| 12 | | 15.8 | 11.9 | 6.3 | 2.6 | 6.4 | 1.06 | 0.50 |

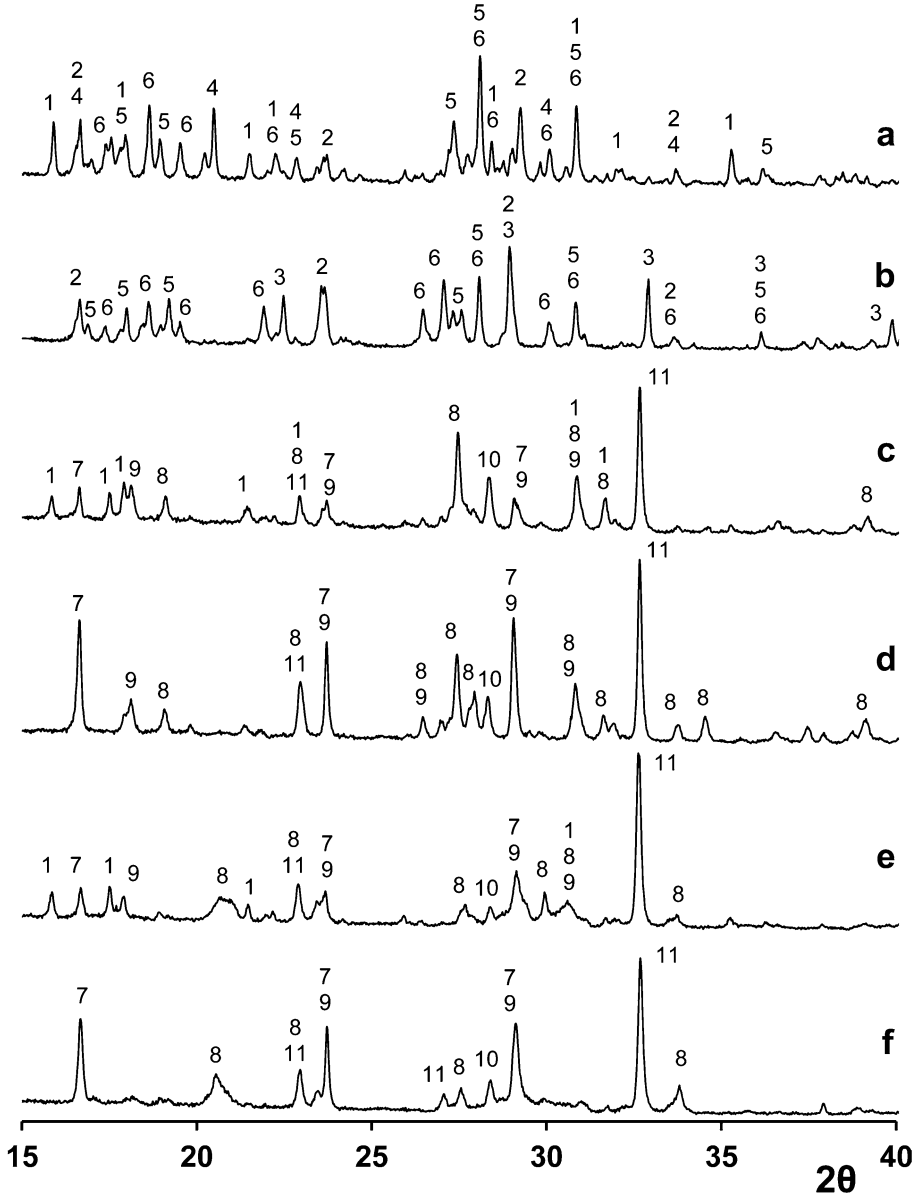


**Fig. 1** X-ray patterns of the fertilizer samples: **a**—*1*, **b**—*2*, **c**—*3*, **d**—*4*, **e**—*5*, **f**—*6*; *1* $(NH_4)_2HPO_4$, *2* $NH_4H_2PO_4$, *3* $NH_4NO_3$, *4* $(NH_4)_2SO_4$, *5* $2NH_4NO_3{\cdot}(NH_4)_2SO_4$, *6* $3NH_4NO_3{\cdot}(NH_4)_2SO_4$, *7* $(NH_4,K)H_2PO_4$, *8* $(NH_4,K)NO_3$, *9* $(NH_4,K)_2SO_4$, *10* KCl, *11* $NH_4Cl$, *2θ* Bragg angle (degree)

X-ray patterns for the samples of grades 16:16:16 and 22:11:11 demonstrate the presence of solid solutions $(NH_4,K)NO_3$, $(NH_4,K)H_2PO_4$ and $(NH_4,K)_2SO_4$, as well as of $NH_4Cl$ and KCl. For samples 3 and 5, the presence of $(NH_4)_2HPO_4$ was established.

Comparing X-ray patterns for the samples 3 and 4 of grade 16:16:16 and 5 and 6 of grade 22:11:11 shows that the intensity of the main diffraction peak of $NH_4Cl$ decreases with a higher degree of ammoniation. This is associated with a reduction of the original content of AN in the composition of samples that results in reducing the amount of $NH_4Cl$ produced in reaction (2).

X-ray patterns for sample 1 of 26:13:0 grade demonstrate the presence of $(NH_4)_2HPO_4$, $NH_4H_2PO_4$, $(NH_4)_2SO_4$, $2NH_4NO_3{\cdot}(NH_4)_2SO_4$ and $3NH_4NO_3{\cdot}(NH_4)_2SO_4$ and for the sample 2 the presence of $NH_4NO_3$, $NH_4H_2PO_4$, $2NH_4NO_3{\cdot}(NH_4)_2SO_4$ and $3NH_4NO_3{\cdot}(NH_4)_2SO_4$.

Comparing X-ray patterns for samples 1 and 2 of grade 26:13:0 demonstrates that the composition of sample 2 has the unbound AN, which could not fully converted to $2NH_4NO_3{\cdot}(NH_4)_2SO_4$ and $3NH_4NO_3{\cdot}(NH_4)_2SO_4$ due to a high content of AN and a low content of $(NH_4)_2SO_4$ in the composition of the fertilizer. This may lead to significant deterioration of the properties of sample 2 compared with sample 1.

All these compounds are typical for complex AN-based fertilizers that is noted in [1, 3, 4, 12].

## Derivatographic analysis

Figures 2, 3, 4 and 5 show the results of the derivatographic analysis for samples 1, 2, 3 and 4. Analysis of curves of the differential thermal analysis (DTA) and of the differential thermogravimetric analysis (DTG) confirms the data of X-ray diffraction analysis.

Curves of the differential thermal analysis (DTA) for 22:11:11 samples are characterized by the following peaks: the reverse phase transition of $(NH_4,K)NO_3$ in

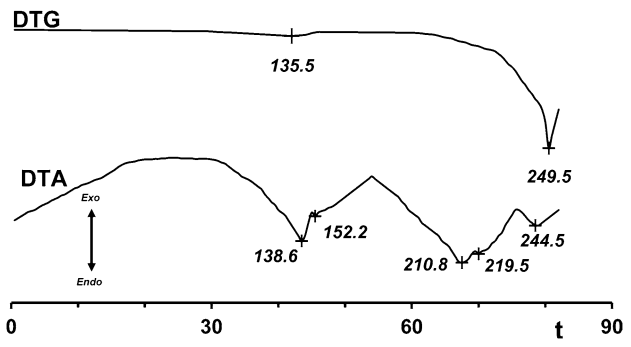


**Fig. 2** *Curves* of the differential thermal analysis (DTA) and of the differential thermogravimetric analysis (DTG) of sample 1: *t* time (min)

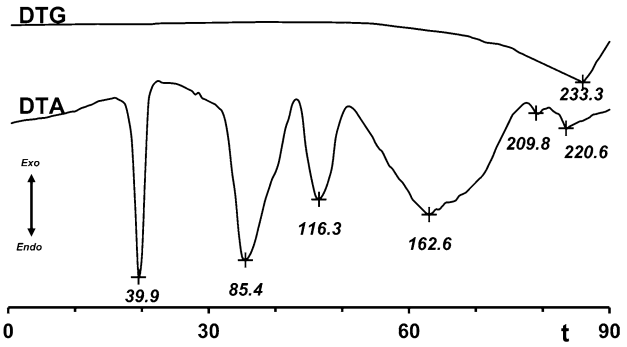


**Fig. 3** *Curves* of the differential thermal analysis (DTA) and of the differential thermogravimetric analysis (DTG) of sample 2: *t* time (min)

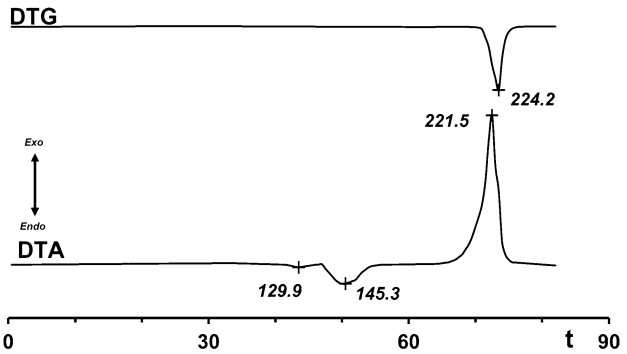


**Fig. 4** *Curves* of the differential thermal analysis (DTA) and of the differential thermogravimetric analysis (DTG) of sample 3: *t* time (min)

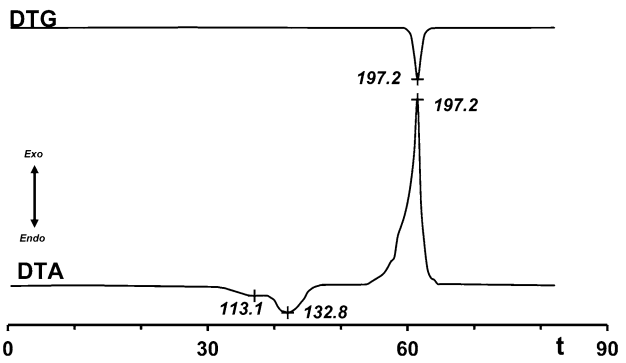


**Fig. 5** *Curves* of the differential thermal analysis (DTA) and of the differential thermogravimetric analysis (DTG) of sample 4: *t* time (min)

$NH_4NO_3{\cdot}2KNO_3$ (113.1 and 129.9 °C, respectively) [15]; melting (132.8 and 145.3 °C) [15]; the exothermal decomposition of the product including the decomposition of $NH_4NO_3$ [15], the polycondensation of $(NH_4,K)H_2PO_4$ and the decomposition of $(NH_4)_2HPO_4$ for samples 3 and 4 (197.2 and 221.5 °C [13].

It can be concluded by comparing the DTG and DTA curves that sample 3 has the higher thermal stability as

compared to sample 4, which may be related to a lower content of AN and a higher content of $(NH_4)_2HPO_4$. It is also worth noting that there is no peak characteristic for the $(NH_4)_2HPO_4$ decomposition in the DTA and DTG curves of sample 3, which would be in the range of 120–200 °C. It may be assumed that its absence is due to the interaction between $(NH_4)_2HPO_4$ and $HNO_3$, which is formed as the result of the partial dissociation of $NH_4NO_3$, according to the reaction:

$$(NH_4)_2HPO_4 + HNO_3 \rightarrow NH_4H_2PO_4 + NH_4NO_3. \quad (6)$$

The decomposition of $(NH_4)_2HPO_4$ is apparently to occur at higher temperatures due to the course of reaction (6). In the case of sample 3, this process takes place in the intensive exothermal decomposition of the product.

At heating sample 2, the peaks are observed on the DTA curve, which is related to the following phenomena: the reverse phase transition of AN IV → III (39.9 °C) [13]; the reverse phase transition of AN III → II (85.4 °C) [13]; the reverse phase transition of AN II → I (116.3 °C) [13]; melting and partial decomposition of adducts $2NH_4NO_3$-$(NH_4)_2SO_4$ and $3NH_4NO_3$·$(NH_4)_2SO_4$ (162.9 °C) [16]; the polycondensation of $NH_4H_2PO_4$ (209.8 °C) [13]; the AN decomposition (220.6 °C) [13].

There are no peaks, which are characteristic to AN in the DTA curve of sample 1. The thermal decomposition of this sample is characterized by the following processes: the decomposition of $(NH_4)_2HPO_4$ (138.6 °C) [13]; the melting and partial decomposition of adducts $2NH_4NO_3$-$(NH_4)_2SO_4$ and $3NH_4NO_3$·$(NH_4)_2SO_4$ (152.2 °C) [16]; the polycondensation of $NH_4H_2PO_4$ (210.8 °C) [13]; the AN decomposition (219.5 °C) [13]; the $(NH_4)_2SO_4$ decomposition (244.5 °C) [14].

It can be concluded when compared the DTG and DTA curves that the presence of $(NH_4)_2HPO_4$ as a part of sample 1 leads to the fact that at temperatures over 100 °C $(NH_4)_2HPO_4$ decomposes to $NH_4H_2PO_4$ to release $NH_3$ into a gas phase. However, sample 2 exhibits the higher thermo-stability than sample 1 when further heated.

It should also be noted that the decomposition of samples 1 and 2 takes place endo-thermally as opposed to samples 3 and 4, whose decomposition proceeds with the release of the large amount of heat. This is due to the absence of chlorine compounds in the composition of samples 1 and 2, which are capable to accelerate the exothermal AN and complex AN-based fertilizers decomposition [7–9, 15].

## Hygroscopicity, caking and static strength

Table 2 presents the results of studying hygroscopicity, caking and static strength of the fertilizer samples obtained.

The presented data show that for the same grade of the fertilizer the increase of *M* reduces the hygroscopicity and caking; however, the static strength of granules decreases also. The reduction of hygroscopicity can be associated with a reduced content of AN, which is highly hygroscopic. The reduction of caking can also be associated with a reduced ammonium chloride content with increasing *M*, which is apparent from intensity of peaks for $NH_4Cl$ in the presented X-ray patterns [1, 18]. The reduction of static strength of granules can be the result of lower strength of phase contacts between granules with increase of *M* in the granulation process [19].

The maximum difference in hygroscopicity and caking is observed for 26:13:0 grade, which can be due to the presence of AN in sample 2, whereas in sample 1 AN is connected in double salts $(NH_4)_2SO_4$·$2NH_4NO_3$ and $(NH_4)_2SO_4$·$3NH_4NO_3$. The minimum difference in hygroscopicity and caking is observed for 27:6:6 grade, which can be explained by the high content of nitrate nitrogen in both samples and the small difference in its content between them.

**Table 2** Hygroscopicity, caking and static strength of granulated fertilizer samples

| Sample no. | Grade | *K*, mmole $g^{-1}$ $h^{-1}$ | $\sigma \times 10^{-2}$, kPa | *P*, MPa |
|---|---|---|---|---|
| 1 | 26:13:0 | 3.21 ± 0.13 | 3.00 ± 0.13 | 2.44 ± 0.14 |
| 2 | | 5.30 ± 0.20 | 4.47 ± 0.18 | 3.70 ± 0.20 |
| 3 | 22:11:11 | 4.04 ± 0.19 | 3.54 ± 0.19 | 3.16 ± 0.19 |
| 4 | | 5.00 ± 0.20 | 4,10 ± 0.30 | 4.40 ± 0.30 |
| 5 | 16:16:16 | 3.04 ± 0.12 | 1.76 ± 0.16 | 5.00 ± 0.30 |
| 6 | | 3.51 ± 0.17 | 3.10 ± 0.30 | 5.10 ± 0.30 |
| 7 | 20:10:10 | 3.74 ± 0.17 | 2.97 ± 0.15 | 2.39 ± 0.15 |
| 8 | | 4.06 ± 0.15 | 3.90 ± 0.20 | 3.80 ± 0.20 |
| 9 | 19:9:19 | 3.22 ± 0.15 | 2.59 ± 0.10 | 3.28 ± 0.19 |
| 10 | | 3.96 ± 0.11 | 3.36 ± 0.16 | 4.40 ± 0.20 |
| 11 | 27:6:6 | 5.00 ± 0.10 | 3.90 ± 0.30 | 3.90 ± 0,20 |
| 12 | | 5.16 ± 0.12 | 4.40 ± 0.30 | 4.90 ± 0.30 |

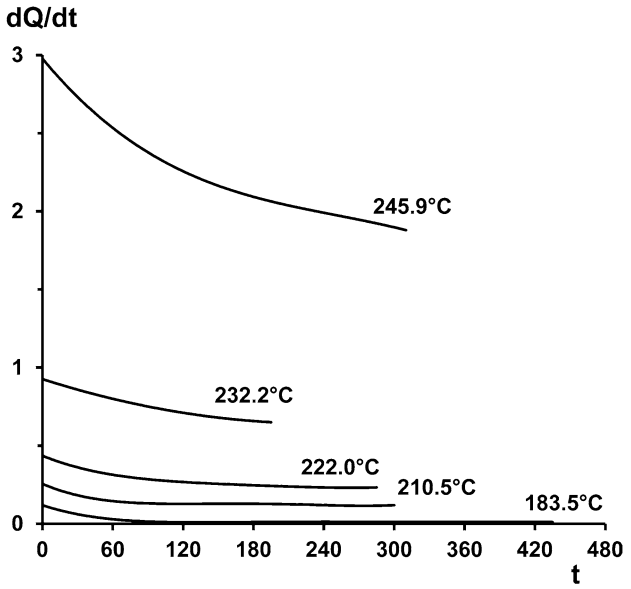


**Fig. 6** Dependence of the heat release rate d$Q$/d$t$ (mW g$^{-1}$) on time $t$ (min) in the thermal decomposition of sample 3

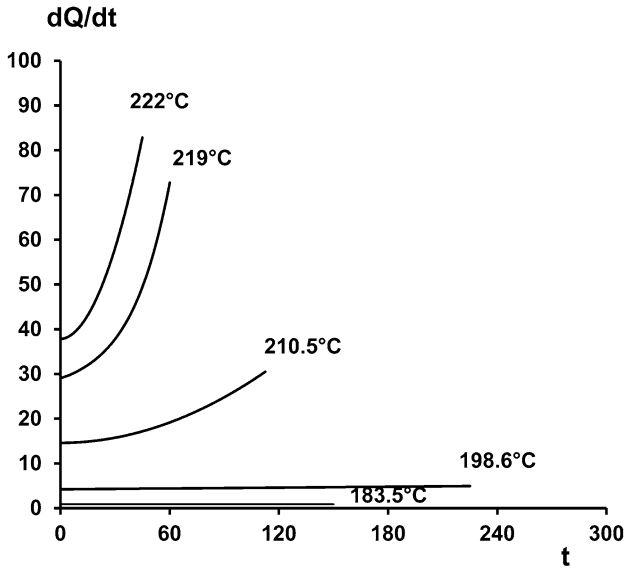


**Fig. 7** Dependence of the heat release rate d$Q$/d$t$ (mW g$^{-1}$) on time t (min) in the thermal decomposition of sample 4

It should also be noted that the highest increase of the caking was observed for 16:16:16 grade ($\sigma_6/\sigma_5 = 1.76$), whereas for the other grades this ratio is much lower. This is possible due to the high ratio of the content of $NH_4Cl$ in two samples of 16:16:16 grade and almost twofold increase in the content of AN in sample 6 when $M$ simultaneously reduced. The closest value to this one is $\sigma_2/\sigma_1 = 1.49$ for 26:13:0 grade. The high ratio $\sigma_2/\sigma_1$ for 26:13:0 grade is apparently due to the fact that in sample 2 the part of NA presents in the free form, while in sample 1 NA is fully bound in double salts.

## Microcalorimetry

Figures 6 and 7 show the curves of the heat release rate dependence on time in the thermal decomposition of samples 3 and 4 in the temperature range of 183.5–245.9 °C.

As indicated above, chloride-anions $Cl^-$ contained in samples under study are catalysts of the AN decomposition, and their catalytic effect increases with the increase of the content of nitric acid in the system and virtually does not occur when its content is low. The accelerating action of $Cl^-$ in the AN decomposition is related to accumulation of nitryl chloride $NO_2Cl$, nitrosyl chloride NOCl and chlorine $Cl_2$ in the system, being more effective oxidizers of ammonium cation $NH_4^+$ and ammonia as compared to nitric acid. The presence of $NH_4H_2PO_4$, $(NH_4)_2HPO_4$ and $(NH_4)_2SO_4$ together with $Cl^-$ reduces $Cl^-$ catalytic effect in AN decomposition.

The study of the heat release rate for sample 4 revealed its low thermal stability. In the decomposition of sample 4 $Cl^-$ accelerating action prevails over decreasing the AN decomposition rate in response to $H_2PO_4^-$, $HPO_4^{2-}$ and $SO_4^{2-}$ anions and, therefore, the decomposition of this sample occurs with the self-acceleration.

Sample 3 has a lower content of AN as compared to sample 4, herewith in its composition a large portion of $H_2PO_4^-$ is substituted with $HPO_4^{2-}$. Anion of $HPO_4^{2-}$ is capable to a higher degree to reduce the concentration of undissociated nitric acid, and so to increase the thermal stability of sample 3. Besides, the content of $(NH_4)_2SO_4$ in sample 3 is also higher than in sample 4. All this contributes to the fact that the accelerating action of $Cl^-$ is not detected, and the decomposition occurs without self-acceleration. Thus, sample 3 has significantly higher thermal stability as compared to sample 4.

Besides the study of the fertilizer samples, the heat release rate was also measured as a function of time in the thermal decomposition of nitrate–phosphate–ammonium slurries at obtaining sample 3 with $M = 1.0$ (sample 3a) and $M = 1.4$ (sample 3b) with humidity of about 8% mass in the temperature range of 243.5–277.0 °C (Figs. 8, 9).

The study of the heat release rate for these samples revealed their high thermal stability, while sample 3b was more thermally stable than sample 3a, which can be explained by the higher content of $(NH_4)_2HPO_4$ in it.

Figure 10 shows the temperature dependencies of the initial heat release rates $(dQ/dt)_{t=0}$ in the thermal decomposition of samples 3, 4, 3a and 3b in Arrenius coordinates. For comparison, Fig. 5 also illustrates the temperature dependence of the initial heat release rates in the AN thermal decomposition studied previously [20].

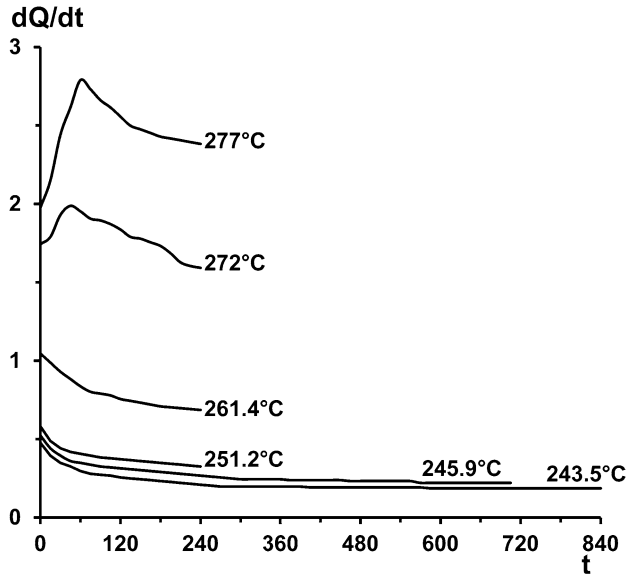


**Fig. 8** Dependence of the heat release rate d$Q$/d$t$ (mW g$^{-1}$) versus time $t$ (min) in the thermal decomposition of sample 3a

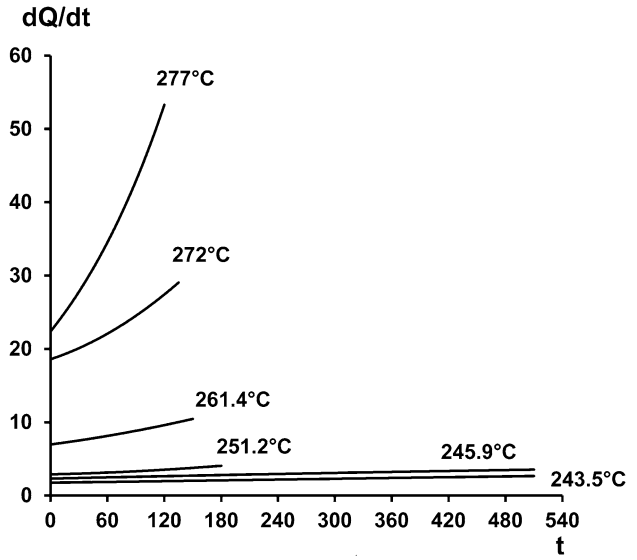


**Fig. 9** Dependence of the heat release rate d$Q$/d$t$ (mW g$^{-1}$) versus time $t$ (min) in the thermal decomposition of sample 3b

The equations of the obtained dependence of $(\mathrm{d}Q/\mathrm{d}t)_{t=0}$ (mW g$^{-1}$) on temperature ($K$) are as follows:

for sample 3

$$\left(\frac{\mathrm{dQ}}{\mathrm{d}t}\right)_{t=0} = 10^{11.7\pm0.7}\exp\left(-\frac{(17.2\pm0.8)\times10^3}{T}\right), \quad (7)$$

for sample 4

$$\left(\frac{\mathrm{dQ}}{\mathrm{d}t}\right)_{t=0} = 10^{18.1\pm0.7}\exp\left(-\frac{(22.3\pm0.9)\times10^3}{T}\right), \quad (8)$$

for sample 3a

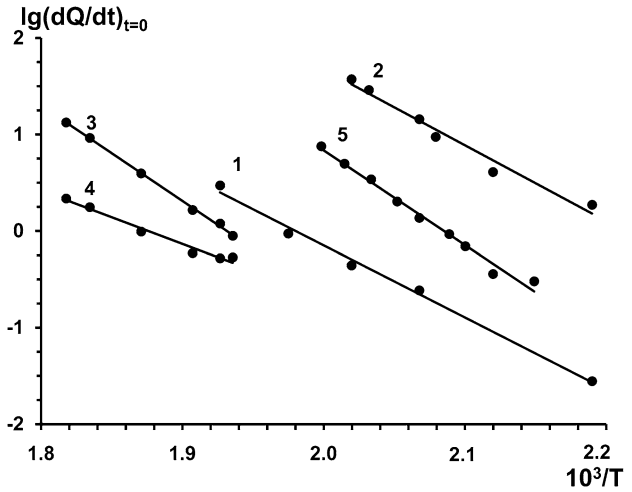


**Fig. 10** Dependence of lg[d$Q$/d$t$ (mW g$^{-1}$)]$_{t=0}$ on $10^3/T$ (K$^{-1}$) for samples 3 (*1*), 4 (*2*), 3a (*3*), 3b (*4*) and ammonium nitrate (*5*)

$$\left(\frac{\mathrm{dQ}}{\mathrm{d}t}\right)_{t=0} = 10^{16.1\pm0.3}\exp\left(-\frac{(22.8\pm0.4)\times10^3}{T}\right), \quad (9)$$

for sample 3b

$$\left(\frac{\mathrm{dQ}}{\mathrm{d}t}\right)_{t=0} = 10^{7.3\pm0.8}\exp\left(-\frac{(12.7\pm0.9)\times10^3}{T}\right). \quad (10)$$

The dependencies presented in Figs. 6, 7, 8, 9 and 10 show that the initial heat release rate of sample 4 is on average by 1–2 orders higher than that for sample 3. Herewith the initial heat release rate of sample 4 significantly exceeds that of AN, while for sample 3 the situation is inverse. Samples 3a and 3b have even higher thermal stability as compared to sample 3, which may be explained by lack of $Cl^-$ in their composition and the high water content.

In any real conditions of conducting the discussed reaction, the thermal explosion is only possible when the values of external parameters of the process exceed the critical ones for the thermal explosion, but calculation of the critical conditions for a real complex production process is a very time-consuming task, and the adiabatic induction period of thermal explosion $\tau_{ad}$ is calculated simply. If the value $\tau_{ad}$ is much greater than the real time of the production process at an appropriate temperature, then the thermal explosion will not occur, and in any real process conditions the induction period may only be greater than under adiabatic conditions. However, if the value $\tau_{ad}$ and process real time are close enough or if $\tau_{ad}$ is even less, it is necessary to calculate the critical conditions of the thermal explosion (the critical temperature for the actual size of the unit and the conditions of heat transfer from it). Only these calculations can give final decision on possibility of the thermal explosion in the process considered.

Calculation of the adiabatic induction period is the most simple and available method to assess the possibility of the thermal explosion for any particular composition. In the complete absence of heat removal (adiabatic conditions) and at a sufficiently high value of the process heat, the thermal explosion will always occur; besides, the degree of conversion in the reaction discussed during induction period will be very small, because all the heat is used for heating a substance. As far as there is no heat removal, the adiabatic induction period is independent of the sample mass and heat removal conditions and it is considered as a characteristic for a substance or mixture discussed. In the theory of thermal explosion because of the weak influence of the process acceleration, the exact quantitative equation for calculating the adiabatic induction period was obtained only for zero-order reaction, and the reaction rate change in the subsequent stages is assumed to have a very small action on the adiabatic induction period [21]:

$$\tau_{ad} = \frac{c_p}{Q_0 k_0} \cdot \frac{RT_0^2}{E} \cdot \exp\left(\frac{E_c}{RT_0}\right), \quad (11)$$

where $c_p$ is the heat capacity of the sample; $Q_0$ is the total process heat; $k_0$ and $E_c$ are the pre-exponential factors and the activation energy of the decomposition rate constant; $T_0$ is the absolute temperature of the decomposition; $R = 8.314$ J mole$^{-1}$ K$^{-1}$ is the universal gas constant.

When $\left(\frac{dQ}{dt}\right)_{t=0} = Q_0 k_0 \exp\left(-\frac{E}{RT_0}\right)$ Eq. (11) takes the following form:

$$\tau_{ad} = \frac{RT_0^2}{E} \cdot \frac{c_p}{\left(\frac{dQ}{dt}\right)_{t=0}}. \quad (12)$$

The results from paper [12] were used to determine the heat capacity of samples under study, provided that in a first approximation the heat capacities of samples 3, 4 and 3a, 3b are equal in pairs. The value of the AN heat capacity was taken according to the data in [2]. The $\tau_{ad}$ values obtained are given in Table 3. The $\tau_{ad}$ values for the same initial temperature may be considered as the characteristics of a relative explosion risk of a substance. The adiabatic induction periods of the thermal explosion for samples 3, 3a and 3b are greater than that for AN, and for sample 4 they are almost by an order less, which reveals the potential danger of thermal spontaneous ignition of the sample during production operations at high temperatures.

## Gravimetric study of the thermal decomposition

The study of the mass loss in the thermal decomposition was carried out for samples 3 and 4 at temperatures of 170, 180, 190 and 200 °C. In addition to the study of the mass loss, the release of ammonium nitrogen, nitrate nitrogen, chlorine and fluorine to the gas phase was also evaluated. The research results are presented in Figs. 11, 12 and 13.

The decomposition intensity for sample 4 is much higher than that for sample 3. The release of chlorine, fluorine, ammonium nitrogen, and nitrate nitrogen from sample 4 to the gas phase is also much more intensive than that from sample 3. Ammonium nitrogen in the initial decomposition stage is released from sample 3 in a greater quantity than that from sample 4. It is related to the higher content of $(NH_4)_2HPO_4$, which starts to decompose in $NH_3$ and $NH_4H_2PO_4$ at low temperatures.

It is also worth mentioning that the maximum amount of fluorine released into the gas phase for both samples is almost the same. It is related to the fact that fluorine in both samples according to [22] is present in the form of compounds $(NH_4)_2SiF_6$, $NH_4F$, $NH_4NO_3{\cdot}(NH_4)_2SiF_6$, $KNO_3$-$K_2SiF_6$, $(NH_4)_2SiF_6{\cdot}NH_4F$, etc., the decomposition of which depends only on the process temperature. The higher fluorine release rate for sample 4 is related to the more intense exothermal decomposition of this sample.

For chlorine, the release into the gas phase depends on the content of AN, so for sample 4 a significantly greater amount of chlorine is released into the gas phase than for sample 3.

The release of chlorine, fluorine, nitrous gases and ammonium compounds into the gas phase leads to the essential complication and more expensive purification of

**Table 3** Adiabatic induction period of the thermal explosion $\tau_{ad}$ of samples 3, 4, 3a and 3b and AN depending on temperature $T$

| $T$, K | $\tau_{ad}$, $h$ | | | | |
|---|---|---|---|---|---|
| | Sample 3 | Sample 4 | Sample 3a | Sample 3b | Ammonium nitrate |
| 473 | 94.64 | 1.50 | 226.83 | 232.00 | 11.38 |
| 478 | 68.04 | 0.97 | 146.60 | 180.92 | 7.00 |
| 483 | 49.29 | 0.63 | 95.69 | 142.00 | 4.35 |
| 488 | 35.97 | 0.42 | 63.05 | 112.02 | 2.73 |
| 493 | 26.45 | 0.28 | 41.94 | 88.90 | 1.73 |
| 498 | 15.58 | 0.19 | 28.14 | 70.94 | 1.11 |
| 503 | 14.59 | 0.13 | 19.05 | 56.90 | 0.72 |
| 508 | 10.94 | 0.09 | 13.01 | 45.88 | 0.47 |

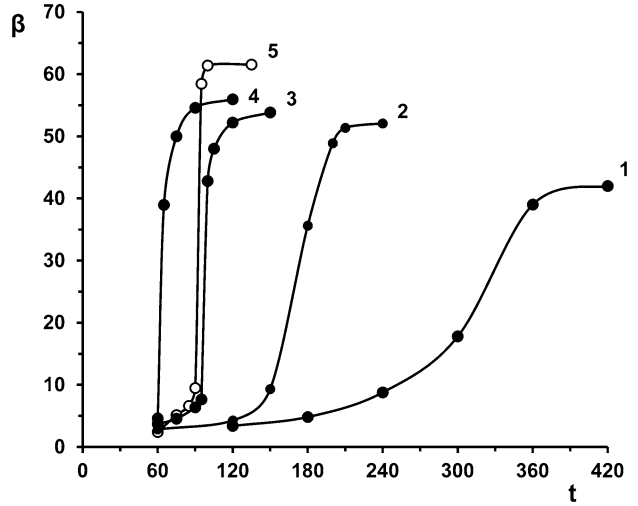


**Fig. 11** Dependence of thermal decomposition degree $\beta = (m - m_0)/m_0 \cdot 100$ (%) versus time $t$ (min) for samples 3 and 4 at constant temperature; sample 3: *1* 170 °C, *2* 180 °C, *3* 190 °C, *4* 200 °C; sample 4: *5* 180 °C

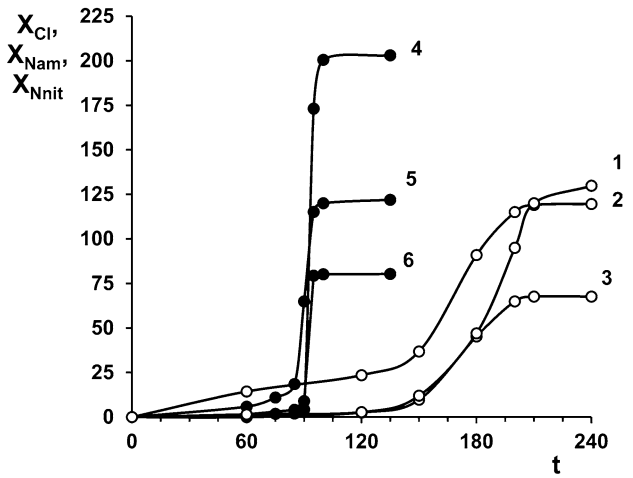


**Fig. 12** Release of chlorine $X_{Cl}$, ammonium $X_{Namm}$ and nitrate nitrogen $X_{Nnitr}$ (g kg$^{-1}$) into the gas phase in the thermal decomposition of samples 3 and 4 at temperature of 180 °C versus time $t$ (min); sample 3: curve *1* Cl, *2* $N_{am}$, *3* $N_{nit}$; sample 4: curve *4* Cl, *5* $N_{am}$, *6* $N_{nit}$

exhaust gases from them, as well as to the more intense corrosion of equipment.

## Dynamic viscosity

The study of dynamic viscosity was performed for ammonium–phosphate–nitrate slurries obtained at production of 22:11:11 grade when $M = 1.7$. To obtain such slurries, phosphoric and nitric acids were mixed in the ratio $P_2O_5$:$HNO_3$ = 0.36:1 (by mass.) and ammoniated up to the specified value of $M$.

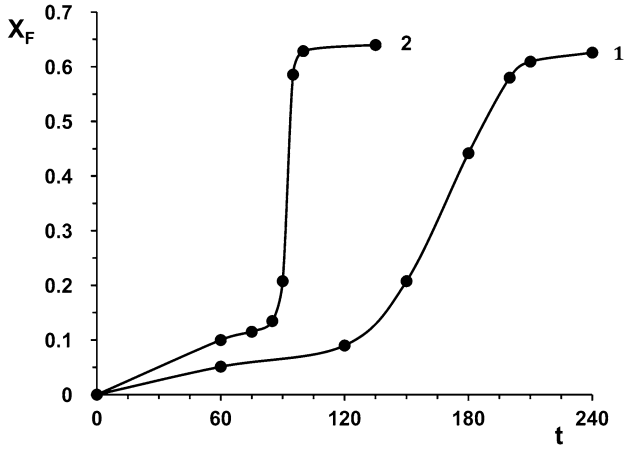


**Fig. 13** Release of fluorine into the gas phase $X_F$ (g kg$^{-1}$) in the thermal decomposition of samples 3 (*curve 1*) and 4 (*curve 2*) at temperature 180 °C versus time $t$ (min)

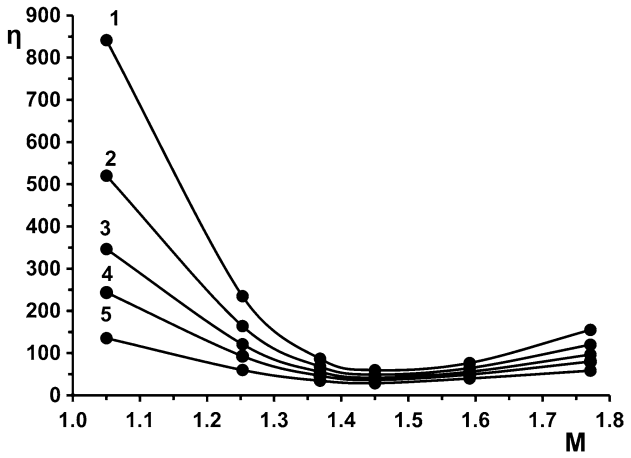


**Fig. 14** The dependence of dynamic viscosity $\eta$ (mPa s) of ammonium–phosphate–nitrate slurry on $M$ at temperature 110 °C and for different values of humidity: *1* 5% mass., *2* 6% mass., *3* 7% mass., *4* 8% mass., *5* 10% mass

Figure 14 shows the dependence of dynamic viscosity of such slurry on $M$ for different values of humidity at 110 °C. The slurry viscosity is apparent to reach the minimum value at $M = 1.45$ for all the values of humidity.

It should be mentioned that the same behavior of viscosity was observed for phosphate ammonia slurries obtained from various types of a phosphate raw [3, 23]. The presence of minimum in the viscosity curve is probably due to the high solubility of ammonium phosphates at $M = 1.4$–$1.5$. The presence in the slurry of impurities of iron, aluminum, magnesium, fluorine, silicon, etc. leads to increasing viscosity due to the formation of poorly soluble compounds [3, 24, 25].

Figures 15 and 16 show the dependences of the slurry dynamic viscosity (for $M = 1.05$ and $M = 1.45$) on humidity at different temperatures. The figures show that

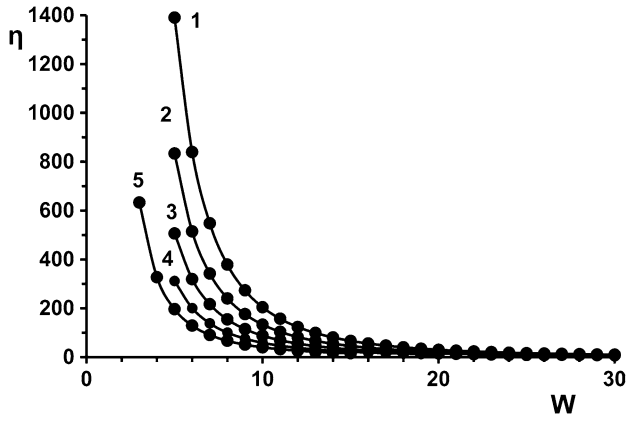


**Fig. 15** Dependence of dynamic viscosity $\eta$ (mPa s) of ammonium–phosphate–nitrate slurry for $M = 1.05$ on humidity (%mass.) for different values of temperature: *1* 100 °C, *2* 105 °C, *3* 110 °C, *4* 115 °C, *5* 120 °C

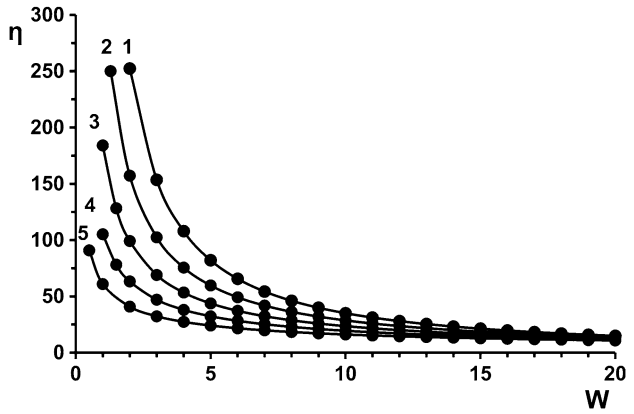


**Fig. 16** Dependence of dynamic viscosity $\eta$ (mPa s) of ammonium–phosphate–nitrate slurry for $M = 1.45$ on humidity (%mass.) for different values of temperature: *1* 100 °C, *2* 105 °C, *3* 110 °C, *4* 115 °C, *5* 120 °C

the slurry viscosity increases with decreasing humidity. Herewith for the slurries at $M = 1.05$, a more rapid increase of viscosity with decreasing humidity is observed.

Temperature influence on dynamic viscosity of the slurries obeys the law of Arrhenius–Andrade [26]:

$$\eta = A_{\exp}\left(\frac{E_v}{RT}\right), \tag{13}$$

where $A$ is the pre-exponential factor and $E_v$ is the activation energy for viscous flow.

Table 4 presents the equations of dynamic viscosity dependence on temperature at the different values of humidity for slurries studied. As can be seen from the equations presented, the activation energy of a viscous flow, the values of pre-exponential factor and the value of dynamic viscosity of the slurry for $M = 1.45$ are substantially less than for $M = 1.05$.

Using the slurries having higher mobility and flowability during their processing in the granular product can significantly reduce the energy costs for the removal of moisture from the granules and reduce the amount of the recirculated product obtainable by a recycle method.

## Conclusions

On the basis of the studies performed, it has been found that increasing the degree of phosphoric acid ammoniation with $M = 1.0$–$1.1$ to $M = 1.6$–$1.7$ influences on the properties of the complex AN-based NP and NPK fertilizers.

It has been shown by X-ray diffraction and derivatographic analysis that the composition of NPK fertilizer (16:16:16 and 22:11:11) contains $(NH_4,K)H_2PO_4$, $(NH_4,K)_2SO_4$, $(NH_4,K)NO_3$, KCl and $NH_4Cl$. When $M = 1.6$–$1.7$, $(NH_4)_2HPO_4$ presents also additionally. The composition of NP fertilizer (26:13:0) contains $NH_4H_2PO_4$, $2NH_4NO_3{\cdot}(NH_4)_2SO_4$ and $3NH_4NO_3{\cdot}(NH_4)_2SO_4$. When $M = 1.0$–$1.1$, $NH_4NO_3$ presents additionally in the system, when $M = 1.6$–$1.7$, $(NH_4)_2HPO_4$ and $(NH_4)_2SO_4$ present additionally.

It is found that the decomposition of NPK fertilizers occurs with the strong exothermal effect and NP fertilizers decomposition occurs with the endothermal effect. The strong exothermal effect of the thermal NPK fertilizer

**Table 4** Equations of dynamic viscosity (mPa·s) dependence for ammonium phosphate nitrate slurries for $M = 1.05$ and $M = 1.45$ for the various humidity values $W$ (% mass.)

| W | $M = 1.05$ | $M = 1.45$ |
|---|---|---|
| 5 | $\eta = 10^{-13.6\pm0.6}\exp\left(\frac{(14.7\pm0.6)\times10^3}{T}\right)$ | $\eta = 10^{-8.5\pm0.4}\exp\left(\frac{(9.0\pm0.4)\times10^3}{T}\right)$ |
| 10 | $\eta = 10^{-11.7\pm0.6}\exp\left(\frac{(11.9\pm0.6)\times10^3}{T}\right)$ | $\eta = 10^{-5.1\pm0.2}\exp\left(\frac{(5.7\pm0.3)\times10^3}{T}\right)$ |
| 15 | $\eta = 10^{-10.6\pm0.5}\exp\left(\frac{(10.5\pm0.4)\times10^3}{T}\right)$ | $\eta = 10^{-3.03\pm0.13}\exp\left(\frac{(3.7\pm0.1)\times10^3}{T}\right)$ |
| 20 | $\eta = 10^{-9.8\pm0.3}\exp\left(\frac{(9.6\pm0.3)\times10^3}{T}\right)$ | $\eta = 10^{-1.59\pm0.02}\exp\left(\frac{(2.4\pm0.1)\times10^3}{T}\right)$ |
| 25 | $\eta = 10^{-9.2\pm0.3}\exp\left(\frac{(9.0\pm0.3)\times10^3}{T}\right)$ | $\eta = 10^{-0.47\pm0.01}\exp\left(\frac{(1.30\pm0.05)\times10^3}{T}\right)$ |

decomposition is associated with the presence of chlorine-contained compounds.

It has been shown that hygroscopicity and caking for 26:13:0, 22:11:11, 16:16:16, 20:10:10, 19:9:19 and 27:6:6 grades decrease by increasing M from 1.0–1.1 to 1.6–1.7.

The study of the thermal decomposition by the example of 22:11:11 grade has demonstrated that increasing the degree of ammonization up to the specified values increases the thermal stability and reduces the intensity of the release of compounds of chlorine, fluorine and nitrous gases into the gas phase.

The study of thermal and rheological properties of ammonium–phosphate–nitrate slurries has allowed to set their high thermal stability, which increases with the increase of the phosphoric acid ammoniation degree. The viscosity of the slurries changes extremely having the minimum value at $M = 1.4–1.5$ and the maximum value at $M = 1.0$. The viscosity of the slurries increases with decreasing moisture content and decreases with increasing temperature according to the law of Arrhenius–Andrade.

**Compliance with ethical standards**

**Conflict of interest** The authors declare no competing financial interest.



## References

1. Kuvshinnikov IM (1987) Mineral fertilizers and salts: properties and methods of their improvement. Khimiya, Moscow
2. Olevskiy VM (1978) Ammonium nitrate technology. Khimiya, Moscow
3. Kononov AV, Sterlin VN, Evdokimova LI (1988) Principles of technology of complex fertilizers. Khimiya, Moscow
4. Shmulyan EK, Portnova NL, Doroshina TV, Abashkina TF, Vinnik MM (1975) Determination of ammonium nitrate phosphate fertilizers and intermediate products composition in the process of nitric-sulfuric decomposition of Karatau rock phosphates. Byulleten Techniko-Ekonomicheskoi Informacii NIITEKHIMa 8:18–23
5. Rubtsov YI, Strizhevsky II, Kazakov AI, Andrienko LP, Moshkovich EB (1989) Possibility of reduction of thermal decomposition rate for ammonium nitrate. J Appl Chem-USSR 62:2169–2174
6. Kazakov AI, Ivanova OG, Kurochkina LS, Plishkin NA (2011) Kinetics and mechanism of thermal decomposition of ammonium nitrate and sulfate mixtures. Russ J Appl Chem 84:1516–1523. doi:10.1134/S1070427211090102
7. Keenan AG, Dimitriades B (1962) Mechanism for the chloride-catalyzed thermal decomposition of ammonium nitrate. J Chem Phys 37:1583–1586. doi:10.1063/1.1733343
8. Rubtsov YI, Strizhevsky II, Kazakov AI, Moshkovich EB, Andrienko LP (1989) Kinetic mechanism of influence of $Cl^-$ on thermal decomposition of ammonium nitrate. J Appl Chem-USSR 62:2417–2422
9. Rubtsov YI, Kazakov AI, Nedelko VV, Shastin AV, Larikova TS, Sorokina TV, Korsounskii BL (2008) Thermolysis of ammonium nitrate/potential donor of active chlorine compositions. J Therm Anal Calorim 93:301–309. doi:10.1007/s10973-007-8868-z
10. Chatterjee SK (1990) Experience with production of urea-based high-grade NPK fertilizers, urea-based NPK plant design and operating alternative: workshop proceedings. International Development Centre, Muscle Shoals, pp 14–20
11. Ranadurai S (1990) Operation experiences with NP-NPK granulation of coromandel fertilizers. Urea-based NPK plant design and operating alternative: workshop proceedings. International Development Centre, Muscle Shoals, pp 21–26
12. Borisov VM, Azhikina YV, Galtsov AV (1983) Physics and chemistry of phosphoric fertilizers production. Reference book, Khimiya
13. Zaitsev PM, Tavrovskaya AY, Podlesskaya AV, Portnova NL (1982) Thermal stability of mineral fertilizer components. Report 1. Nitrates, chlorides, fluorides, fluorine silicates, ammonium, potassium, calcium, aluminum and iron phosphates. Trudy NIUIFa 240:154–167
14. Tavrovskaya AY, Podlesskaya AV, Portnova NL (1982) Thermal stability of mineral fertilizer components. Report 2. Ammonium, potassium, calcium, aluminum and iron phosphates. Magnesium compounds. Trudy NIUIFa 240:168–185
15. Tavrovskaya AY, Portnova NL, Abashkina TF (1976) Thermographic study of ammonium nitrate phosphate fertilizer. Byulleten Techniko-Ekonomicheskoi Informacii NIITEKHIMa 7:10–14
16. Babkina TS, Golovina NB, Bogachev AG, Olenev AV, Shevelkov AV, Uspenskaya IA (2012) Crystal structures and physicochemical properties of mixed salts of ammonium nitrate and sulfate. Russ Chem B 61:3339. doi:10.1007/s11172-012-0005-x
17. Galperin LN, Kolesov YR, Mashkinov LB, Terner YE (1973) Differential automatic calorimeters (DAC) of different purpose. Book of reports from VI USSR conference on calorimetry. Inorganic Chemistry and Electrochemistry Institute of GSSR Academy of Sciences, Tbilisi, pp 539–543
18. Walker GM, Magee TRA, Holland CR, Ahmad MN, Fox JN, Moffat NA, Kells AG (1998) Caking process in granular NPK fertilizer. Ind Eng Chem Res 37:435–438. doi:10.1021/ie970387n
19. Shchukin ED, Amelina EA (2003) Surface modification and contact interaction of particles. J Dispers Sci Technol 24:377–395. doi:10.1081/DIS-120021796
20. Rubtsov YI, Kazakov AI, Morozkin SY, Andrienko LP (1984) Kinetics of heat release at thermal decomposition of commercial ammonium nitrate. J Appl Chem-USSR 57:1926–1929
21. Frank-Kamenetskiy DA (1987) Diffusion and heat exchange in chemical kinetics. Nauka, Moscow
22. Tavrovskaya AY, Portnova NL, Abashkina TF, Zaitsev PM (1977) Thermographic study of fluorine silicate compounds contained in ammonium nitrate phosphate fertilizer. Trudy NIUIFa 231:184–194
23. Akiyama T, Ando J (1972) Constituents and properties of ammoniated slurry from wet-process phosphoric acid. B Chem Soc Jpn 45:2915–2920. doi:10.1246/bcsj.45.2915
24. Zhong B, Li J, Xiang Zhang Y, Liang B (1999) Principle and technology of ammonium phosphate production from middle-quality phosphate ore by a slurry concentration process. Ind Eng Chem Res 38:4504–4506. doi:10.1021/ie980419m
25. Campbell GR, Leong YK, Berndt CC, Liow JL (2006) Ammonium phosphate slurry rheology and particle properties—the

influence of Fe(III) and Al(III) impurities, solid concentration and degree of neutralization. Chem Eng Sci 61:5856–5866. doi:10.1016/j.ces.2006.05.010

26. Barnes HA (2000) Handbook of elementary rheology. University of Wales Institute of Non-Newtonian Fluid Mechanicsm, Aberystwyth